JOURNAL OF MATERIALS SCIENCE 22 (1987) 663–669

Probabilistic aspects of strength of short-fibre composites with planar fibre distribution

ROBERT C. WETHERHOLD
Department of Mechanical and Aerospace Engineering, State University of New York at Buffalo, Buffalo, New York 14260, USA

The study of the fracture of short-fibre composites must involve statistics as an integral part. Two components of composite strength, each with probabilistic aspects, are described in this paper: fibre crossover reinforcement, and fibre gap bridging before fracture. The fibre crossover density is proposed as a measure of mutual fibre strengthening, and simulations are performed to estimate this density. Several different fibre orientations are proposed which have identical elastic properties but different crossover densities, indicating that more information is required for strength prediction than for elastic property prediction. The crossover density is a random variable whose average increases roughly as a fibre length squared function, and whose coefficient of variation decreases with increasing fibre length. The phenomenon of fibres bridging microcracks is also examined as a fracture mechanism for fibres whose length well exceeds their critical length. General probabilistic expressions are derived which give the distribution of the number of fibres bridging a gap perpendicular to the applied load. These formulae are applied to the distribution of strength of an aligned fibre system.

1. Introduction

Mechanical properties of composites can be broadly divided into two categories: thermoelastic properties, and strength properties. A variety of different approaches have been used for employing micromodels to predict the thermoelastic properties of short-fibre composites. Often regular arrays of fibres are assumed, in contrast to the actual arrays as seen through photomicrographs. These assumptions seem to work well, however, since elastic constants are the result of an averaging process. The calculation of elastic properties thus tends to be fairly robust with respect to the assumptions employed. The strength properties of composites, however, depend on stochastic microscopic events typical of a brittle material. The distribution of strength thus requires careful physical modelling combined with a statistical approach. The fracture process depends on point, not average phenomena. Additional information is likely to be required for strength prediction, which information is not required for thermoelastic property prediction.

A variety of approaches have been advanced to predict the strength of short-fibre composites [1–17]. The great majority of these papers [1–14] attempt to predict strength as a single-valued variable, ignoring the inherent statistical nature of strength. In addition, the theoretical models advanced are almost always restricted to two specialized fibre orientation states: completely aligned, and completely random. The most common analysis used is the "laminate analogy", a constant-strain model for the composite constituents. For thermoelastic properties of a material with either continuous or very high aspect ratio reinforcement, this analogy gives good results. For strength properties, the relative locations of weak and strong volumes are clearly important to composite strength. The strength properties can thus clearly not be treated as single-valued variables without loss of valuable physical insight.

For the case of fibre-dominated fracture, the initial probabilities of fibre fracture depend on the elastic solution for fibre loads. Although no closed-form solution is available, a photoelastic study [18] has indicated that local reinforcement may be provided by fibres crossing over each other. This has the effect of lowering fibre load, hence lowering the probability of fracture. An analogous effect of crossed fibres providing greater strength has been observed in continuous-fibre composites [19–21] and will be commented on later in this paper. This localized strengthening effect is an example of information required for a strength analysis, but not for an elastic property analysis. In the first part of this paper, the effect of fibre crossover density is explored using a simulation method.

As the composite specimen progresses toward final fracture, the action of fibres bridging a microcrack becomes important. These microcracks are formed during fabrication [22], and may be expected to grow and coalesce during progressive fracture [23, 24], resulting in a critical damage zone or gap at final fracture. The strength of the fibres at any given cross-section depends on their number, strength distribution, and interaction. A general theory involving all of these variables is not available; however, the more variables which may be considered probabilistically, the greater the understanding of the overall process of strength variability. In the second part of this paper, general

0022–2461/87 $03.00 + .12

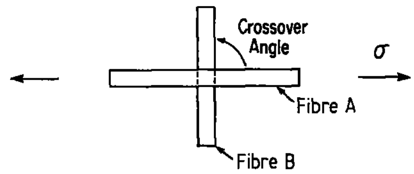

Figure 1 Fibre crossover.

methods are developed for the number of fibres crossing a plane or bridging a gap perpendicular to the applied load. The developed methods are then applied to the particular cases of aligned and random fibre distributions.

2. Fibre crossover and reinforcement

The arrangement of fibres may have an influence on strength by offering local reinforcement at fibre crossover points. According to a photoelastic study by McGarry and Fujiwara [18], the stress in a longitudinal fibre is decreased in the vicinity of a neighbouring fibre which crosses above or below it (see Fig. 1); (as the crossover fibre B becomes aligned with longitudinal fibre A, the effect on fibre A may change from local reinforcement to more general load sharing). The stress reduction in the crossover fibres will depend on the vertical distance between the fibres. However, since no closed-form or numerical solutions for this stress reduction are available, we will consider only an average crossover effect.

If the fibre strength is statistically distributed according to a Weibull distribution, the action of this crossover reinforcement may be easily seen. The probability of failure F of a fibre under a far-field stress $\sigma = \varepsilon/E_f$ (applied strain/fibre modulus) may be given [25] by

$$F(\sigma) = 1 - \exp\left[-\int_v \left(\frac{\sigma t}{\sigma_0}\right)^{\alpha} \mathrm{d}V\right] \qquad (1)$$

where (α, σ_0) are Weibull (shape, location) parameters, $\mathrm{d}V$ = fibre volume element = $(\pi/4)d_f^2\mathrm{d}x$ and t = geometric locus to account for deviations from far-field stress σ.

Since the values of α are typically greater than 10, the impact of a local stress reduction ($t < 1$) from crossover is great. The reinforced crossover region contributes little to the probability of failure. This reduction in failure probability will also occur if the longitudinal fibre is not perfectly aligned with the load. The number of crossover points should thus have a direct effect on the fracture of fibre-dominated composites.

The stiffness properties of short-fibre composites may be modelled using orientation averaging techniques [26–32]. The effective elastic constants depend on moment-like integrated properties of the fibre orientation distribution. For planar fibre orientations, these effective properties may be expressed [30] as

$$C_{ij} = C^0_{ij} + F(C^0_{ij}, \bar{C}_{ij})f_p + G(C^0_{ij}, \bar{C}_{ij})g_p \qquad (2)$$

where C^0_{ij} are properties for a random state of orientation, $\bar{C}_{ij}$ are certain linear combinations of constituent properties and f_p, g_p are integrated orientation parameters; $f_p = 2\langle\cos^2\phi\rangle - 1$, $g_p = \frac{1}{5}[8\langle\cos^4\phi\rangle - 3]$ and $\langle\cos^n\phi\rangle = \int_{-\pi/2}^{\pi/2}\cos^n\phi\, n(\phi)\mathrm{d}\phi$.

Thus, two different fibre orientation distributions with the same fibre volume fraction may exist which give the same elastic properties; equality of f_p, g_p is sufficient to ensure this. For example, consider two orientation distributions:

$$n_1(\phi) = C_1 - C_2|\phi| \qquad \phi\varepsilon\left[-\frac{\pi}{2}, \frac{\pi}{2}\right] \qquad (3a)$$

$$n_2(\phi) = C_3\delta(0) + C_4\left[\delta\left(\frac{\pi}{4}\right) + \delta\left(\frac{-\pi}{4}\right)\right] \qquad \phi\varepsilon\left[\frac{-\pi}{2}, \frac{\pi}{2}\right] \qquad (3b)$$

Use of the delta function as in Equation 3b denotes that the proportion of fibres at 0° is $C_3/(C_3 + 2C_4)$; the proportion at $\pi/4$ is $C_4/(C_3 + 2C_4)$; the proportion at $-\pi/4$ is $C_4/(C_3 + 2C_4)$. Using the normalization requirement, we generate two equations:

$$\int_{-\pi/2}^{\pi/2} n_i(\phi)\mathrm{d}\phi = 1 \qquad i = 1, 2 \qquad (4)$$

The remaining two equations are derived by setting the expected values of $\cos^2\phi$ and $\cos^4\phi$ equal for the two distributions, i.e.

$$\langle\cos^2\phi\rangle_1 = \langle\cos^2\phi\rangle_2$$
$$\langle\cos^4\phi\rangle_1 = \langle\cos^4\phi\rangle_2 \qquad (5)$$

where $\langle\cos^n\phi\rangle_i = \int_{-\pi/2}^{\pi/2}\cos^n\phi\, n_i(\phi)\mathrm{d}\phi$. This last condition is sufficient and necessary for equality of orientation parameters f_p, g_p, and hence equality of elastic properties, between the two distributions. Solving the linear system given by Equations 4 and 5 for the constants C_i, we find

$$C_1 = \frac{1}{\pi} + \frac{\pi}{8} \doteq 0.711$$
$$C_2 = 1/2$$
$$C_3 = 1/2$$
$$C_4 = 1/4 \qquad (6)$$
$$f_p = 0.50$$
$$g_p = 0.40$$

This indicates a partial alignment of the fibres, with resulting orthotropy of properties.

As another example, consider two members of the class of distributions with quasi-isotropy. For all members of this class, $f_p = g_p = 0$. Following the form for quasi-isotropic laminates, consider the elastically equivalent distributions:

$$n_3(\phi) = \frac{1}{\pi} \qquad \phi\varepsilon[-\pi/2, \pi/2]$$

$$n_4(\phi) = \frac{1}{3}\left[\delta(0) + \delta\left(\frac{\pi}{3}\right) + \delta\left(\frac{-\pi}{3}\right)\right] \qquad (7)$$
$$\phi\varepsilon[-\pi/2, \pi/2]$$

These distributions already satisfy the normalization requirement.

The above orientation distributions may be simulated to determine the average number of crossover points of the fibres. A viewing space was defined, and

TABLE I Fibre crossover number for orthotropic orientations $n_1(\phi)$, $n_2(\phi)$

Fibre length (in.)*	$n_1(\phi)$			$n_2(\phi)$		
	Average	Standard deviation	Coefficient of variation (%)	Average	Standard deviation	Coefficient of variation (%)
0.5	20.0	3.9	19.5	15.3	1.2	7.8
1.0	80.3	8.4	10.5	69.2	6.4	9.2
2.0	306.8	18.4	6.0	292.5	17.5	6.0

*1 in. = 25.4 mm.

the centres of gravity were assigned within the space using a random-number generator. The angles were assigned to ensure the proper number of fibres within defined intervals (continuous distributions) or at given angles (delta function distributions). Continuous distributions used 10° intervals, with those fibres within an interval having the angle of the centre of the interval. Within a 26 in. × 25 in. (660 mm × 635 mm) viewing space, 400 fibres were drawn, and the number of intersections was calculated. Results are given in Tables I and II for an average of six replicates, and sample fibre distributions are shown in Figs 2 to 5.

3. Calculations for bridging fibres

The number of fibres crossing a given plane or bridging a gap perpendicular to the applied load has implications for the strength of the material. This number is a random variable, dependent on the fibre orientation distribution, the fibre length distribution, the spatial distribution of fibre centres of gravity, and the size of the gap. In the following development, the fibre length is assumed constant, based on the relative insensitivity of composite strength to moderate fibre length variation [17]. The number of bridging fibres yields information on composite strength, as indicated by simple rule-of-mixtures calculations [16]. The fibre length is assumed substantially greater than the critical length so that fibres which bridge the developed damage zone or gap will tend to fracture, and not pull out. Fibres which end within the gap are assumed to pull out.

Results are obtained first for an aligned fibre system. Consider a fibre whose centre of gravity (c.g.) is at (X_0, Y_0) with length l. The defined area is $x\varepsilon[0, a]$, $y\varepsilon[0, b]$, with $a, b \gg l$ so that boundary effects may be ignored (see Fig. 6).

The condition for a fibre's crossing a plane $X = A$ may be stated as

$$P\left[X_0 + \frac{l}{2} \geqslant A \cap X_0 - \frac{l}{2} \leqslant A\right]$$

or

$$P\left[A - \frac{l}{2} \leqslant X_0 \leqslant A + \frac{l}{2}\right] \quad (8)$$

where X_0 = random variable of x-location of fibre c.g. Assuming a uniform, homogeneous fibre distribution, the fibre c.g. density function f_{x_0} is

$$f_{x_0}(x) = \frac{1}{a} \qquad x\varepsilon(0, a) \quad (9)$$

This yields an expression for a fibre's crossing the plane, which is independent of plane location A:

$$P[\text{fibre crosses plane } x = A] = \int_{A-l/2}^{A+l/2} f_{x_0}(x)\,\mathrm{d}x = \frac{l}{a} \quad (10)$$

Similarly, the probability of a fibre's bridging a gap βl beginning at $x = A$ may be stated as

$$P[\text{fibre bridges gap } \beta l]$$
$$= P\left[X_0 + \frac{l}{2} \geqslant A + \beta l \cap X_0 - \frac{l}{2} \leqslant A\right]$$
$$= P\left[A - \frac{l}{2} + \beta l \leqslant X_0 \leqslant A + \frac{l}{2}\right] \qquad \beta < 1$$
$$= \frac{l}{a}(1 - \beta) \quad (11)$$

The probability of a fibre's crossing a plane or bridging a gap may also be derived for a non-aligned planar system (see Fig. 7). The probability of crossing a plane $x = A$ is given by

$$P[\text{fibre crosses plane } x = A]$$
$$= P\left[X_0 + \frac{l}{2}\cos\phi \geqslant A \cap X_0 - \frac{l}{2}\cos\phi \leqslant A\right]$$
$$\phi\varepsilon\left(-\frac{\pi}{2}, \frac{\pi}{2}\right) \quad (12)$$

To illustrate the solution for this case, consider a

TABLE II Fibre crossover number for isotropic and quasi-isotropic orientations $n_3(\phi)$, $n_4(\phi)$

Fibre length (in.)*	$n_3(\phi)$			$n_4(\phi)$		
	Average	Standard deviation	Coefficient of variation (%)	Average	Standard deviation	Coefficient of variation (%)
0.5	24.0	4.2	17.5	18.5	1.8	9.7
1.0	98.3	12.6	12.8	83.2	8.8	10.6
2.0	379	27.1	7.2	341.3	12.9	3.8

*1 in. = 25.4 mm.

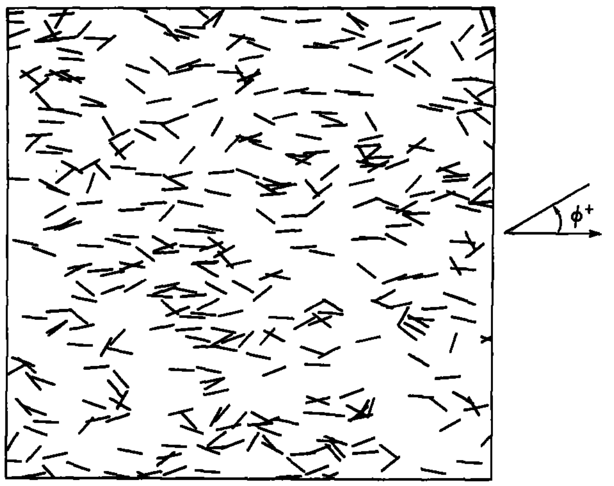

Figure 2 Simulated fibre distribution for $n_1(\phi)$.

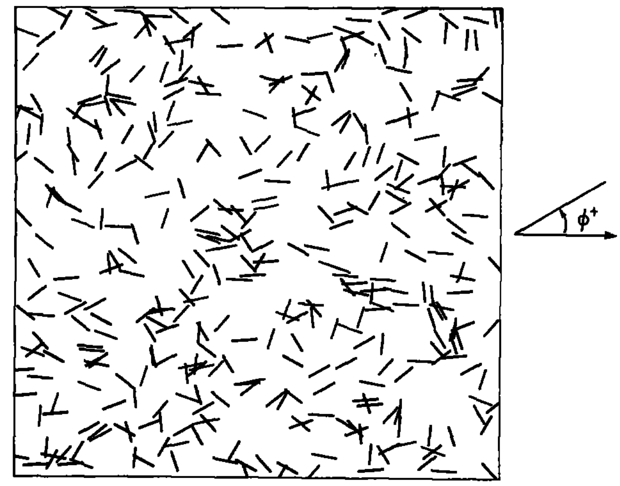

Figure 4 Simulated fibre distribution for $n_3(\phi)$.

uniform orientation and location distribution:

$$f_{x_0}(x) = 1/a \qquad x\varepsilon(0, a)$$
$$f_\phi(\phi) = 1/\pi \qquad \phi\varepsilon\left(\frac{\pi}{2}, \frac{\pi}{2}\right) \tag{13}$$

Using standard methods for functions with non-unique inverses [33], the density and distribution functions for the random variable $Z = (l/2)\cos\phi$ are given by

$$f_z(z) = \frac{2}{\pi}\left[\left(\frac{l}{2}\right)^2 - z^2\right]^{-1/2} \qquad z\varepsilon\left(0, \frac{l}{2}\right)$$
$$F_z(z) = \frac{2}{\pi}\left[\cos^{-1}\left(\frac{2z}{l}\right) + \frac{\pi}{2}\right] \tag{14}$$
$$\cos^{-1}\left(\frac{2z}{l}\right)\varepsilon\left(0, -\frac{\pi}{2}\right)$$

The desired probability (Equation 12) of crossing a plane thus becomes

$$P[X_0 + Z \geqslant A \cap X_0 - Z \leqslant A] = \int_{\text{Area}} f_{xz}(x, z)\,\mathrm{d}x\mathrm{d}z \tag{15}$$

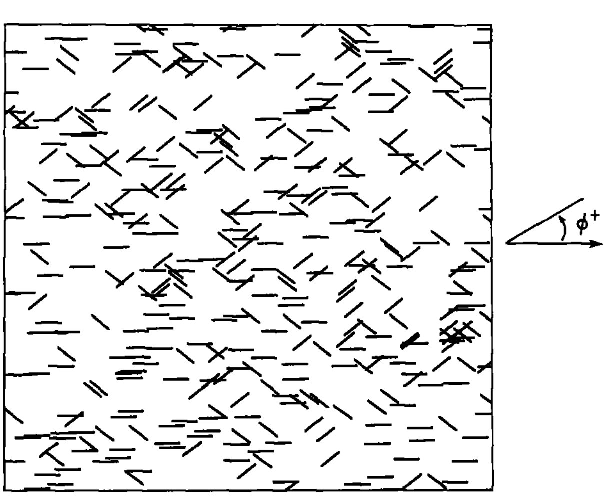

Figure 3 Simulated fibre distribution for $n_2(\phi)$.

The area of integration is that satisfying the left-hand side of Equation 15, subject to the domains of definition of X, Z. We assume independence of X and Z, that is, location and angle, to solve Equation 15 as

$$\int_{z=0}^{l/2}\int_{x=A-z}^{A+z}\frac{1}{a}\,\mathrm{d}x\,\frac{2}{\pi}\left[\left(\frac{l}{2}\right)^2 - z^2\right]^{-1/2}\mathrm{d}z = \frac{2l}{\pi a} \tag{16}$$

The number of fibres bridging a cross-section of width βl starting at $x = A$ gives a similar result for uniform distributions of location and angle given by Equation 13:

$$P[\text{fibre bridges gap } \beta l]$$
$$= P\left[X_0 + \frac{l}{2}\cos\phi \geqslant A + \beta l \cap X_0 - \frac{l}{2}\cos\phi \leqslant A\right] \tag{17}$$
$$= P[X_0 + Z \geqslant A + \beta l \cap X_0 - Z \leqslant A] \qquad \beta < 1$$
$$= \frac{2\beta l}{\pi a}\cos^{-1}\beta + \frac{2l}{\pi a}(1 - \beta^2)^{1/2}$$
$$\cos^{-1}\beta\varepsilon\left(0, -\frac{\pi}{2}\right)$$

Note that Equations 10, 11, 16 and 17 are insensitive to the particular value of cross-section A, as expected. This is in keeping with our assumption of a spatially stationary process (Equation 9).

The above Equations 11 and 17 give the probability for a fibre crossing a gap. The probability that n fibres out of N total will cross a gap is thus given by the binomial distribution

$$P[n \text{ fibres bridge gap}] = \binom{N}{n}p^n(1 - p)^{N-n}$$
$$0 \leqslant n \leqslant N \tag{18}$$

where p is the gap crossing probability for an individual

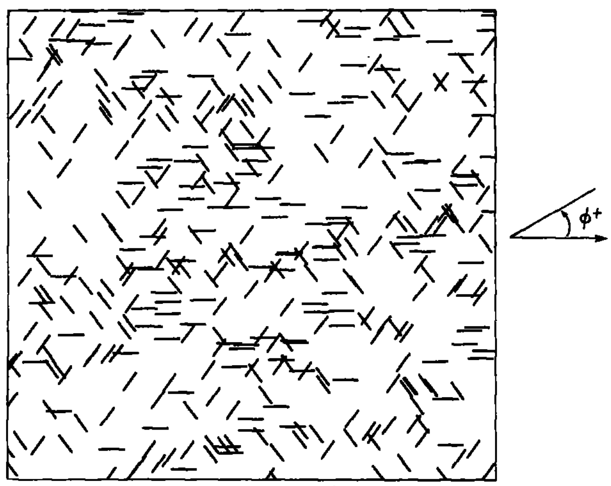

Figure 5 Simulated fibre distribution for $n_4(\phi)$.

fibre. For large N, n, this calculation may be replaced by the Poisson distribution [34]

$$P[n \text{ fibres bridge gap}] \doteqdot \frac{\mu^n e^{-\mu}}{n!} \tag{19}$$

where $\mu = Np$.

4. Discussion and conclusions

The effect of fibre crossover should increase composite strength due to providing local reinforcement for stressed fibres. It is possible to have different fibre orientations with the same elastic properties but different crossover densities, hence different strengths. The density of crossovers will depend on fibre orientation, fibre length and number of fibres, and will itself be a random variable. A numerical simulation has been carried out to determine the sensitivity of fibre crossover to the fibre length and orientation.

The dependence of crossover on fibre length may be seen to be roughly a length squared function; i.e. doubling fibre length will increase fibre crossover density by a factor of four. It may also be seen that the coefficient of variation (COV) of fibre crossover density generally decreases with increasing fibre length. This points to a lessening of variability of this strengthening mechanism with increasing fibre length.

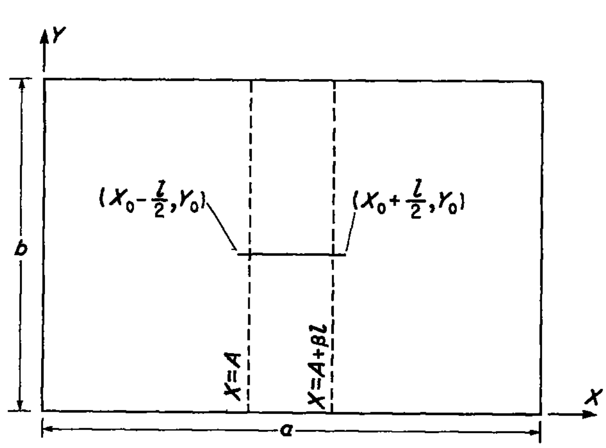

Figure 6 Geometry of aligned fibre.

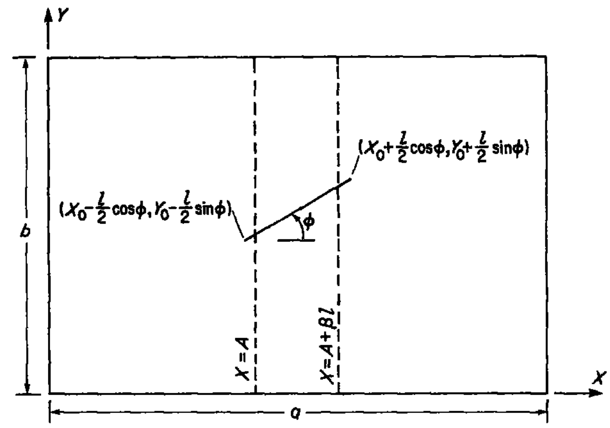

Figure 7 Geometry of non-aligned fibre.

The particular orientation distribution chosen is seen to have an impact on crossover density and its COV. For the 1/2 in. (13 mm) fibre length, we may achieve a 31% increase (for $n_1(\phi)$ compared with $n_2(\phi)$) or 30% increase (for $n_3(\phi)$ compared with $n_4(\phi)$) in crossover density for identical elastic properties. The COV of the crossover density may also vary from 19.5% to 7.8% for n_1 and n_2, or from 17.5% to 9.7% for n_3 and n_4. The optimization of the strengthening of fibre crossover may then be carried out by considering various distributions with the same integrated properties f_p, g_p, and hence the same elastic properties.

A simple illustrative calculation may serve to illustrate the potential effect of the average crossover number for two different fibre distributions which possess identical elastic coefficients. Consider the random fibre system $n_3(\phi)$ and the quasi-random system $n_4(\phi)$ given by Equation 7. For a representative 1 in. × 1 in. × 0.10 in. thick (25 mm × 25 mm × 2.5 mm thick) composite piece, with volume fraction $V_f = 50\%$, with 16 μm fibres present in bundles containing 150 fibres, each bundle 1 in. (25 mm) long, there are 1078 "fibres" (bundles). Assume that at each crossover point, $t^\alpha \ll 1$ in. Equation 1 so that the crossover region effectively does not contribute to the probability of fracture. Since the true details of t are unknown, let us assume that the reduced fracture probability region extends over (nd_f) where d_f = the bundle diameter. For close packing with the bundle acting in concert as a single unit, its $d_f = 238\,\mu$m. Allowing for a simple weak-link model for damage leading to failure, the ratio of reliabilities for $n_3(\phi)$ and $n_4(\phi)$ are

$$\frac{R_3}{R_4} = \frac{\prod_{i=1}^{N} \exp\left[-L_i(\sigma_{i,3}/\sigma_0)^\alpha\right]}{\prod_{i=1}^{N} \exp\left[-L_i(\sigma_{i,4}/\sigma_0)^\alpha\right]} \tag{20}$$

where N = total number of fibres, $\sigma_{i,k}$ = load in ith fibre for distribution k (k = 3, 4) and L_i = effective fibre length; $L_i = L - j(nd_f)$ where j = number of crossovers for the ith fibre.

For these fibre distributions, the average load carried on a typical fibre may be approximately prorated by $\langle\cos^3\phi\rangle = 0.424$ [17], so that the typical fibre load $\sigma_i = 0.424\,\sigma_{fu}$. If we set $\sigma_{fu} = 200 \times 10^3$ p.s.i.

TABLE III Results of computer simulation

n	R_3/R_4
1	1.019
5	1.096
10	1.202

(1.38 GPa), $\sigma_0 = 220 \times 10^3$ p.s.i. (1.52 GPa) and $\alpha = 10$, then the ratio of the reliabilities at the average failure stress may be calculated from

$$\frac{R_3}{R_4} = \exp\left[2(m_3 - m_4)nd_f\left(\frac{0.424\,\sigma_{fu}}{\sigma_0}\right)^{\alpha}\right] \quad (21)$$

where m_i = number of crossover points for distribution i.

The factor of two arises in Equation 21 since m crossover points affect $2m$ fibres. Actual values of m_i from computer simulation were $m_3 = 239\,685$, $m_4 = 226\,108$ (see Table III for the numerical results). This illustration points to the potential effect of an increase in the number of crossover points. It also expresses the need for greater understanding of the stress locus function t in Equation 1 so that more quantitative results for reliability improvement may be obtained.

Although making no claims that the fracture of continuous and discontinuous fibre composites is identical, it is interesting to note that a similar strengthening effect of crossover fibres has been observed in two studies involving continuous-fibre laminated composites. In a study of tensile strength by Herakovitch [19], the strength of alternating sequence angle-ply laminates $[(\pm\theta)_2]_s$ was greater than that of clustered sequence laminates $[+\theta_2/-\theta_2]_s$. In Herakovitch's study, the action of the alternating layers apparently forced the failure surface to fracture fibres, as opposed to cracking the matrix and delaminating. In addition, a study of rail shear strength by Chang *et al.* [20] showed significant differences in rail shear strength exist for various 0/90 laminates. The shear strength drops by 1/3 when the proportion of 0° plies is increased by 10%, and does not change when the proportion is increased by another 10% (see Table IV) [21]. The dramatic change in shear strength is hard to explain, since a decrease in the proportion of 0° layers (increase in 90° layers) might be expected to modestly increase strength due to the clamping of the 90° fibres (the 0° direction is in the rail direction). Consider instead the number of runs in each laminate sequence, where a run is defined as a continuation of the same orientation in the stacking sequence. The largest number of runs implies the maximum of fibre crossovers, imparting crack-stopping ability to the laminate. The number of runs is given in Table IV, and indicates that fibre crossover is a desirable trait for increased strength.

Expressions have been developed for determining the probability of a fibre's crossing a plane or bridging planes perpendicular to the applied load. These formulations have been applied to the case of an aligned fibre and a random fibre system with N fibres. The distribution of the number of bridging fibres is binomial, and may be approximated by the Poisson distribution for large N. The effect on composite strength may be seen using a rule-of-mixtures approach with an aligned fibre system. Consider a specimen with dimensions $a \times b \times c$ in the x, y, z directions, subjected to a force in the x direction. The volume fraction of fibres, V_f, is related to the total number of fibres N by

$$V_f = \frac{N(\pi/4)d_f^2 l}{abc} \quad (22)$$

The normal rule-of-mixtures approximation for the strength of a composite with long fibres is [16]

$$\sigma_{cu} = \sigma_{fu}V_f + \sigma'_m(1 - V_f) \quad (23)$$

where $(\sigma_{cu}, \sigma_{fu})$ = ultimate tensile strength of (composite, fibre) and σ'_m = matrix stress at ultimate tensile strain of fibres.

The matrix term in Equation 23 is small even before cracking, and matrix cracks or gaps further reduce it, so that it may be ignored [23]. The V_f term in Equation 23 implicitly represents an average number of fibres bridging the fracture zone gap. If N_b represents the number of bridging fibres, the composite ultimate strength for loading in the x direction may be represented by

$$\sigma_{cu} = \sigma_{fu}\frac{\pi}{4}d_f^2\frac{N_b}{bc} \quad (24)$$

Knowing the distribution of N_b will give the distribution of σ_{cu}, assuming that the variability of fibre failure stress is less than the variability of N_b:

$$P[N_b = n] = P\left[\sigma_{cu} = \frac{\sigma_{fu}(\pi/4)d_f^2 n}{bc}\right] \quad (25)$$

This method may also be used to calculate the probability that composite strength lies between certain limits:

$$P\left[\sigma_{cu}\varepsilon\left(\frac{\sigma_{fu}(\pi/4)d_f^2 n_1}{bc}, \frac{\sigma_{fu}(\pi/4)d_f^2 n_2}{bc}\right)\right] = P[N_b\varepsilon(n_1, n_2)] \quad (26)$$

TABLE IV Rail shear strength of symmetric cross-ply laminates

No. of plies	Volume fraction of 0° plies (%)	Stacking sequence	Runs in stacking sequence	No. of replicates	Strength, S_{AVG} (p.s.i.)*
24	50	$[(0/90)_6]_s$	23	2	19480
20	60	$[0, 0, 90, 0, 0, 90, 0, 90, 0, 90]_s$	15	3	12860
20	70	$[0, 0, 90, 0, 0, 90, 0, 0, 90, 0]_s$	13	3	13210

*1 p.s.i. = 6895 Pa.

TABLE V Calculated strength distribution

No. of bridging fibres, n	x (10^3 p.s.i.)*	$P[N_b \leq n] = P[\sigma_{cu} \leq x]$
650	71.3	0.0368
670	73.5	0.1840
690	75.7	0.4930
700	76.8	0.6633
710	77.9	0.8049
730	80.1	0.9583
740	81.2	0.9848

*10^3 p.s.i. = 6.895 MPa.

For illustration, a strength distribution is constructed using the data of Masoumy *et al.* [35] for aligned fibre composites. For 1 in. (25 mm) long fibre bundles composed of 110 fibres of diameter 16 μm at a volume fraction $V_f = 50\%$, the average strength $\bar{\sigma}_{cu}$ is 75×10^3 p.s.i. (517 MPa). The bundle is observed to act in concert as a single fibre [35]. The gauge section has dimensions (a, b, c) of (3 in., 1/2 in., 1/8 in.) (76 mm, 13 mm, 3 mm) [36], giving N, the total number of fibres, to be 2742. Using a first-order approximation for Equation 24 at the average, we have

$$\bar{\sigma}_{cu} \doteq \frac{(Np)A_f\sigma_{fu}}{bc} \tag{27}$$

where A_f = area of fibre bundle, (Np) = average N_b value for a Bernoulli process and p = bridging probability. The fibre strength σ_{fu} is assumed to be 200×10^3 p.s.i. (1.38 GPa). Equations 27 and 11 may be solved for the gap size, which is found to 0.252 in. (6.4 mm). Using this, we may construct a strength distribution (see Table V). Having found an approximate value for the gap size, the prediction of strength distributions at other fibre lengths, volume fractions and orientations is possible. Further exploration of the model predictions at various fibre volume fractions and fibre lengths, for aligned systems with and without fibre strength variability, and the additional development and model exploration for non-aligned systems may be found elsewhere [37, 38].

References

1. H. T. HAHN, in "Composite Materials in the Automobile Industry", edited by S. V. Kulkarni, L. C. H. Zweben and R. B. Pipes (ASME, New York, 1978) p. 85.
2. J. C. HALPIN and J. L. KARDOS, *Polym. Eng. Sci.* **18** (1978) 496.
3. K. L. JERINA and J. C. HALPIN, in Proceedings of 6th Symposium on Composite Materials in Engineering Design, May 1972, St Louis (American Society for Metals, 1973) p. 600.
4. J. L. KARDOS, J. C. HALPIN and S. L. CHANG, in Proceedings of 8th International Congress on Rheology, September, 1980, Naples, Vol. 3 (Plenum Publishing, New York, 1980) p. 255.
5. H. ISHIKAWA, T-W. CHOU and M. TAYA, *J. Mater. Sci.* **17** (1982) 832.
6. C. ZWEBEN, *J. Mech. Phys. Solids* **22** (1974) 193.
7. *Idem, Eng. Fract. Mech.* **6** (1974) 1.
8. D. L. DENTON, in Proceedings of 36th Annual Conference, Reinforced Plastics/Composites Institute, Society of the Plastics Industry, February 1981, Session 16-A, p. 1.
9. H. T. HAHN, in Proceedings of National SAMPE Symposium, May 1979, p. 1470.
10. B. D. AGARWAL and G. S. GIARE, *Mater. Sci. Eng.* **52** (1982) 139.
11. G. A. COOPER, *J. Mater. Sci.* **5** (1970) 645.
12. S. K. GAGGAR and L. J. BROUTMAN, in Proceedings of SPE Engineering Properties and Structures Division, Technical Conference: Additives – their effect on process parameters and product performance, Hudson, Ohio, October 1975 (Society of Plastics Engineers, Greenwich, 1975) p. 146.
13. *Idem*, in Proceedings of 30th Anniversary Technical Conference, Reinforced Plastics/Composites Institute, Society of the Plastics Industry, February 1975, Section 9E, p. 1.
14. C. ZWEBEN and B. W. ROSEN, *J. Mech. Phys. Solids* **18** (1970) 189.
15. M. MIWA, T. OHSAWA and K. TAHARA, *J. Appl. Polym. Sci.* **25** (1980) 795.
16. H. FUKUDA and T-W CHOU, *J. Mater. Sci.* **16** (1981) 1088.
17. *Idem, ibid.* **17** (1982) 1003.
18. F. J. MCGARRY and M. FUJIWARA, *Modern Plastics* (July 1968) 143.
19. C. T. HERAKOVITCH, *J. Compos. Mater.* **16** (1982) 216.
20. F. K. CHANG, R. A. SCOTT and G. S. SPRINGER, *ibid.* **18** (1984) 290.
21. F. K. CHANG, personal communication (1984).
22. K. FRIEDRICH, *Compos. Sci. Tech.* **22** (1985) 43.
23. M. G. BADER, T-W CHOU and J. QUIGLEY, in "New Developments and Applications in Composites", edited by D. Wilsdorf (Met. Soc. AIME, New York, 1979) p. 127.
24. P. T. CURTIS, M. G. BADER and J. E. BAILEY, *J. Mater. Sci.* **13** (1978) 377.
25. W. WEIBULL, *Ingeniörsvetenkaps Akademienhandlingar* Nr 151 (1939).
26. C. D. WU and R. L. MCCULLOUGH, in Developments in Composite Materials, vol. 1, edited by G. S. Holisten (Applied Science, London, 1977) 119.
27. R. M. CHRISTENSEN and F. M. WAALS, *J. Compos. Mat.* **6** (1972) 518.
28. A. GHESQUIERE and J. C. BAUWENS, *J. Appl. Polym. Sci.* **20** (1976) 891.
29. D. C. CHANG and G. J. WENG, *J. Mater. Sci.* **14** (1982) 2182.
30. R. B. PIPES, R. L. MCCULLOUGH and D. G. TAGGART, *Polym. Compos.* **3** (1982) p. 34.
31. S. H. MCGEE, PhD thesis, University of Delaware (1982).
32. R. L. MCCULLOUGH, R. B. PIPES, D. TAGGART and J. MOSKO, in "Composite Materials in the Automobile Industry", edited by S. V. Kulkarni *et al.* (ASME, New York, 1978) p. 141.
33. R. V. HOGG and A. T. CRAIG, "Introduction to Mathematical Statistics", 4th Edn. (Macmillan, New York, 1978) p. 149.
34. T. T. SOONG, "Probabilistic Modeling and Analysis in Science and Engineering", (Wiley, New York, 1981) p. 176.
35. E. MASOUMY, L. KACIR and J. L. KARDOS, *Polym. Compos.* **4** (1983) 64.
36. J. L. KARDOS, private communication (1986).
37. R. C. WETHERHOLD, *Mater. Sci. Eng.* in press.
38. *Idem, ibid.*

Received 13 May 1985
and accepted 6 May 1986